

Color tuning of light-emitting-diodes by modulating the concentration of red-emitting silicon nanocrystal phosphors

G. Barillaro^{a)} and L. M. Strambini

Dipartimento di Ingegneria dell'Informazione, Università di Pisa, via G. Caruso 16, 56122 Pisa, Italy

(Received 10 December 2013; accepted 17 February 2014; published online 3 March 2014)

Luminescent forms of nanostructured silicon have received significant attention in the context of quantum-confined light-emitting devices thanks to size-tunable emission wavelength and high-intensity photoluminescence, as well as natural abundance, low cost, and non-toxicity. Here, we show that red-emitting silicon nanocrystal (SiN) phosphors, obtained by electrochemical erosion of silicon, allow for effectively tuning the color of commercial light-emitting-diodes (LEDs) from blue to violet, magenta, and red, by coating the LED with polydimethylsiloxane encapsulating different SiN concentrations. High reliability of the tuning process, with respect to SiN fabrication and concentration, and excellent stability of the tuning color, with respect to LED bias current, is demonstrated through simultaneous electrical/optical characterization of SiN-modified commercial LEDs, thus envisaging exciting perspectives for silicon nanocrystals in the field of light-emitting applications. © 2014 AIP Publishing LLC. [<http://dx.doi.org/10.1063/1.4867201>]

The research activity into the development of luminescent forms of silicon has now spanned two decades, driven by scientific interest, commercial potential, and technological advancement.¹ It is now well established that silicon crystallites of reduced dimensions, typically below 5 nm, emit light with high efficiency due to quantum confinement effect, with respect to inefficient light emission of bulk crystalline silicon. Canham² was the first to demonstrate in 1990 room-temperature photoluminescence from nanocrystallites of silicon (i.e., porous silicon) that were obtained by electrochemical erosion of crystalline silicon in acidic electrolytes. Many other methods were subsequently developed for the synthesis of luminescent nanostructured forms of silicon, including annealing of SiO_x powder followed by etching in HF,³ plasma synthesis,⁴ solution reduction of SiCl₄,⁵ plasma etching of silicon and subsequent thermal oxidation.⁶

In last two decades, a significant research effort has been paid to the demonstration of electroluminescence properties of silicon nanocrystals (SiNs), as well as to the development of both all-silicon and hybrid light-emitting-diodes (LEDs) exploiting SiNs.^{7–11} However, despite the exceptionally high photoluminescence (PL) efficiency of SiNs,^{9,12,13} electroluminescence efficiencies of SiN-LEDs have been reported to be significantly lower than those obtained using II-VI semiconductors and have not reflected the reported large photoluminescence efficiency values.

Very recently, SiNs with high PL quantum yield (about 17%), obtained by low-cost electrochemical erosion of crystalline silicon substrate, have been proposed as non-toxic phosphors for wavelength conversion in ultraviolet/blue LEDs.^{14,15} Wavelength conversion is a general technique, alternative to color mixing, which involves converting some or all of the LED output wavelengths into different visible wavelengths, with the main aim of achieving white-light LEDs. Ultraviolet/blue light from an LED is used to excite

one or more wavelength converter materials, which are coated on top of the LED, that re-emit on different wavelengths. The balanced mixing of the excitation light with the light re-emitted by the wavelength converter materials results in the appearance of new colors and, possibly, in white light. A number of materials, usually rare-earth phosphors^{16–19} and, more recently, quantum dots^{20–23} have been employed so far as wavelength converters in ultraviolet/blue LEDs. Nonetheless, a major concern of such materials is their toxicity and effect on the environment, which pushes research attention towards the use of alternative materials, as well as to their synthesis/production.

Here, we show that SiN phosphors with strong and broad photoluminescence in the red portion of the spectrum, obtained by electrochemical erosion of silicon, allow for effectively tuning the color of commercial blue-LEDs from blue to violet, magenta, and red via wavelength conversion, by coating the LED with polydimethylsiloxane (PDMS) encapsulating different SiN concentrations. Good reliability of the tuning process, with respect to SiN fabrication and concentration, and excellent stability of the tuning color, with respect to LED bias current, is demonstrated through simultaneous electrical/optical characterization of a number of SiN-modified commercial LEDs. In spite of the huge research effort that has been paid so far to the use of SiNs for LED applications, the possibility of efficiently tuning the color of LEDs via wavelength-conversion by modulating the concentration of red-emitting SiN phosphors has never been reported. New exciting perspectives in the field of light-emitting applications of SiNs are envisaged by building on these results.

Figures 1(a)–1(c) show typical daylight optical pictures of a commercial blue-LED turned-off (a) and turned-on ((b) and (c)), before (b) and after (c) coating of the LED active area with 5 μl of PDMS encapsulating red-emitting SiNs. The color appearance of the light emitted from the LED turns from blue (Fig. 1(b)) to magenta (Fig. 1(c)) thanks to efficient SiN red-light conversion of a portion of the blue-light emitted

^{a)}Electronic mail: g.barillaro@iet.unipi.it. Tel.: +39 050 2217 601. Fax: +39 050 2217 522.

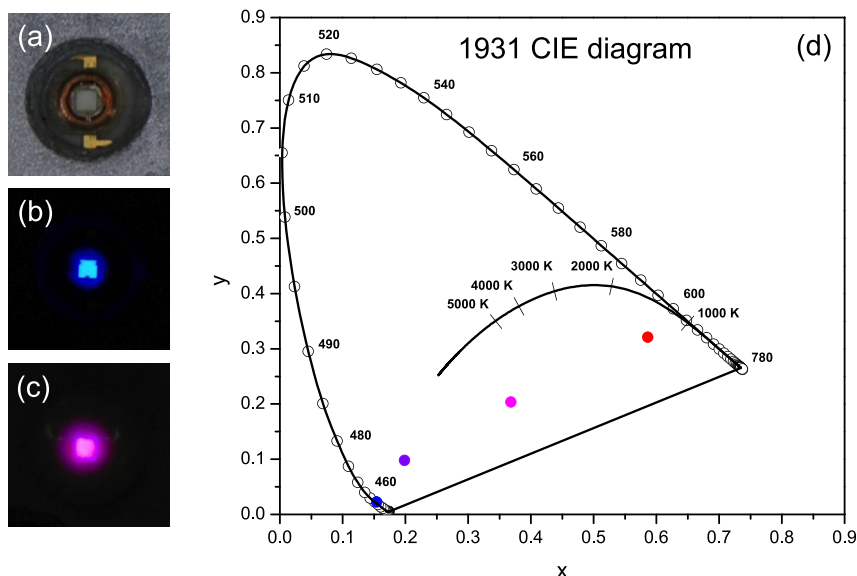


FIG. 1. (a)-(c) Daylight optical pictures of a commercial blue-LED turned-off (a) and turned-on ((b) and (c)), before (b) and after (c) modification with 5 μl of PDMS encapsulating SiNs. Pictures (b) and (c) are taken using an exposure time of 1/125 s with respect to 1/15 s of (a), so as to avoid intensity saturation of the camera when the LED is turned on, which explains the black background in (b) and (c) if compared to (a). (d) Color coordinates (average value and standard deviation) of different LEDs before (blue dot) and after modification with 5 μl of PDMS encapsulating different concentrations of SiNs, namely, low (violet dot), medium (magenta dot), and high (red dot) concentrations.

by the LED. In Figure 1(d), color coordinates x and y (average value and standard deviation, this latter non-visible being smaller than the dots representing the average value) of different LEDs before (blue dot) and after modification with 5 μl of PDMS encapsulating different SiN concentrations, namely, low (violet dot), medium (magenta dot), and high (red dot) are shown on the standard 1931 CIE diagram. As the concentration of SiN increases, the LED color turns from pure blue (unmodified LED, $x = 0.154 \pm 0.0004$, $y = 0.022 \pm 0.0005$) to violet ($x = 0.199 \pm 0.007$, $y = 0.098 \pm 0.004$), magenta ($x = 0.368 \pm 0.005$, $y = 0.203 \pm 0.003$), and red ($x = 0.587 \pm 0.001$, $y = 0.321 \pm 0.004$). Standard deviation values of color coordinates clearly indicated that the tuning process is very reliable with respect to both SiN fabrication and

encapsulation in PDMS. The color coordinates datapoints shift from blue to red remaining on a straight-line, thus suggesting that only the relative intensity between excitation blue-light and down-converted red-light changes with SiN concentration, while the line-shape of the emission spectrum is not significantly affected (as will be here on clarified). This implicitly demonstrates that the produced SiNs exhibit good reliability in terms of luminescent properties and, in turn, nanostructured morphology. The straight line best-fitting the color coordinate datapoints intercepts the white-light line in the region of warm white (about 1000°K), thus suggesting that by further increasing SiN concentration it is feasible to achieve warm white-light. This has noteworthy implications both from research and commercial points of view.

Figure 2(a) shows a schematic representation of the main technological steps required for fabrication of red-emitting SiN phosphors, as well as for preparation of PDMS encapsulating different concentrations of SiNs. Red-emitting SiNs are

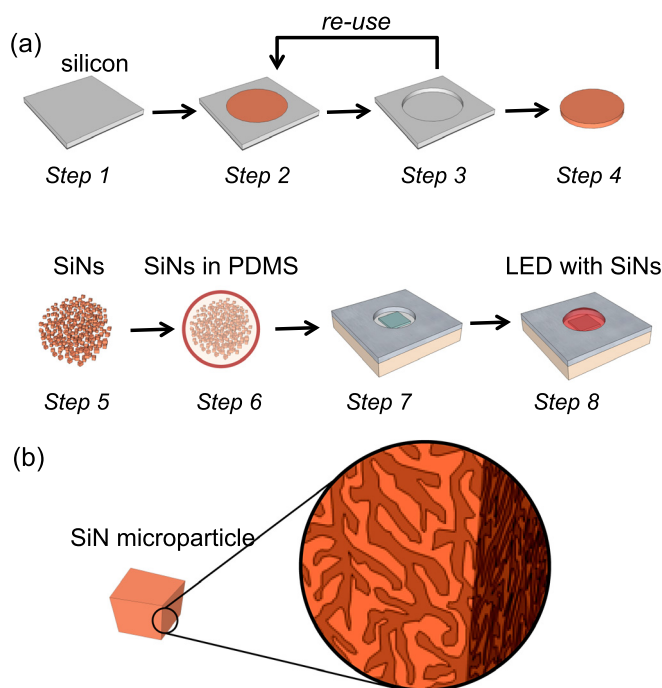


FIG. 2. (a) Sketch of the main technological steps needed for fabrication of the luminescent SiN microparticles and synthesis of the PDMS composites encapsulating SiNs. (b) Sketch of a single SiN microparticle highlighting the nanocrystalline network.

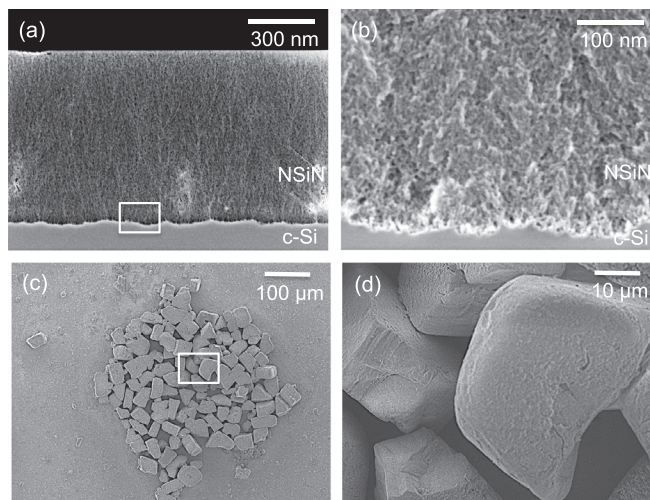


FIG. 3. (a) and (b) SEM cross-sections at two different magnifications—(a) 100 $k\times$ and (b) 500 $k\times$ —of a 1- μm -thick silicon nanocrystal network with porosity of 85%. The nanostructured morphology of the silicon network can be appreciated in (b). (c) and (d) SEM images of a bunch of SiN microparticles at two different magnifications—(c) 10 $k\times$ and (d) 20 $k\times$ —dropped on the clean surface of a silicon die.

prepared by electrochemical etching²⁴ of *p*-type silicon substrates (orientation (100), resistivity $2.5 \div 4.0 \Omega\cdot\text{cm}$, thickness $625 \mu\text{m}$) in acidic electrolytes ($\text{HF}(48\%):\text{ethanol}(99.9\%) = 1:1$ by vol.) using a two-steps process. The electrochemical etching is tuned to produce a network of SiNs with porosity (by definition, the ratio between dissolved and original silicon mass) of about 85% and thickness of $40 \mu\text{m}$ (Fig. 2(a), step 2), in the first phase, and to perform the lift-off of the SiN network from the substrate and obtain a $40\text{-}\mu\text{m}$ -thick free-standing SiN membrane (Fig. 2(a), step 3), in the second phase. In particular, in the first phase, an etching current density $J_w = 300 \text{ mA}/\text{cm}^2$ is applied for 240 s, on the basis of preliminary experiments carried out to obtain relationships between etching current density J and porosity P as well as between etching time t and thickness d of the SiN network (see supplementary material²⁵). The etching current density is then increased to the electropolishing value $J_p = 1260 \text{ mA}/\text{cm}^2$ for 10 s in the second phase. The two-steps process is repeated up to 12 times, thus producing 12 silicon nanocrystal membranes from the same silicon die. Thickness of the SiN membrane is tailored to comply with two opposite needs: increasing mechanical stability to allow the membrane withstanding the liftoff process without breaking; reducing self-absorption of light re-emitted by silicon

nanocrystals when excited with blue-light. Figures 3(a) and 3(b) show typical scanning electron microscope (SEM) cross-sections, at two different magnifications ($100 \text{ k}\times$ and $500 \text{ k}\times$, respectively), of $1\text{-}\mu\text{m}$ -thick silicon nanocrystal network with porosity of 85%. The nanostructured morphology of the silicon nanocrystal network can be appreciated in Fig. 3(b).

Each one of the SiN membranes resulting from the etching process is washed in ethanol and pentane, then all the membranes are collected into a small vial filled with 2 ml of deionized water and sonicated (at 40 kHz) for 4 h to get luminescent SiN microparticles with square-like shape and size of about $40 \mu\text{m} \times 40 \mu\text{m} \times 40 \mu\text{m}$ that can be easily handled for subsequent encapsulation into PDMS (Fig. 2(a), step 5). A sketch of a single SiN microparticle is shown in Fig. 2(b), which also highlights the SiN network. Figures 3(c) and 3(d) show SEM images of a bunch of SiN microparticles, at two different magnifications ($10 \text{ k}\times$ and $20 \text{ k}\times$, respectively), obtained by dropping $1 \mu\text{l}$ of the solution resulting at the end of the sonication process on the clean surface of a silicon die. Good uniformity about size and shape of the SiNs is obtained after sonication. A storage time of a few hours after sonication allows SiN microparticles to deposit at the bottom of the vial. After deionized water is

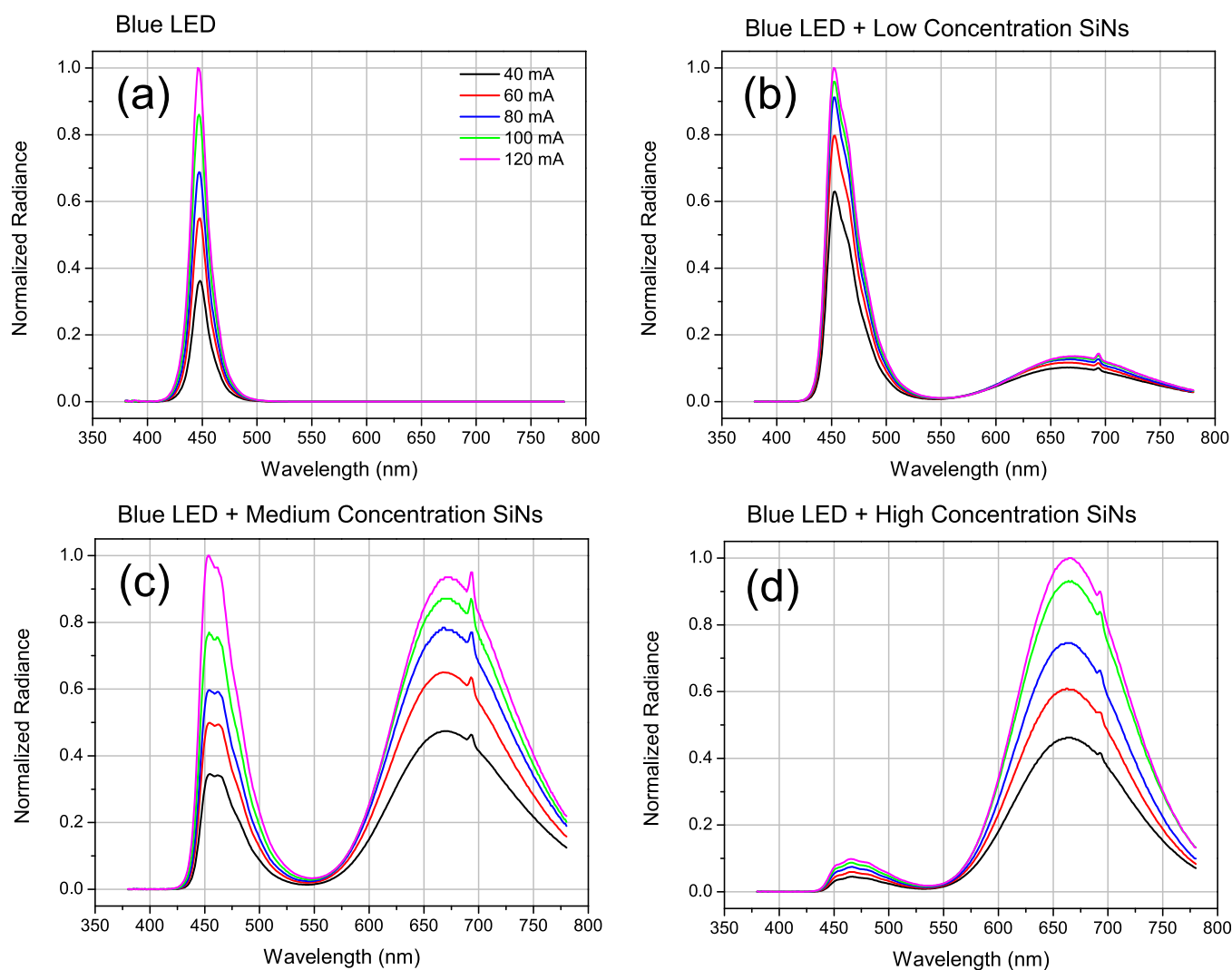


FIG. 4. Typical normalized radiance spectra of commercial blue-LEDs before (a) and after ((b)-(d)) modification with $5 \mu\text{l}$ of PDMS encapsulating different SiN concentrations, as a function of the LEDs bias current.

removed, a powder of SiN microparticles is obtained. The SiN microparticle powder is mixed with PDMS (Fig. 2(a), step 6) with the twofold aim of obtaining a PDMS composite encapsulating SiNs that can be easily and accurately placed on top of commercial LEDs, as well as preventing both aging and degradation of the luminescent particles due to environmental conditions (relative humidity, operation temperature, etc.). PDMS is prepared by Sylgard 184, which features low absorption in the visible region of the electromagnetic spectrum, as well as good stability over time, both in terms of mechanical and chemical properties from -45°C to 200°C . Three PDMS composites encapsulating different concentrations of SiN microparticles, namely, low, medium, and high, are produced to evaluate and quantify the effect of the red-emitting SiNs on both emission spectrum and color of commercial blue-LEDs. PDMS/SiN composites with high, medium, and low SiN microparticle concentrations are prepared using onefold, twofold, fourfold polymer volumes, respectively, to which all SiN microparticles resulting from the whole etching of a single silicon die are mixed with. For each specific SiN concentration, several commercial blue-LEDs (InGaN Venus Blue LED, size $1.14\text{ mm} \times 1.14\text{ mm}$) are modified by dropping $5\ \mu\text{l}$ of the prepared PDMS/SiN composite on top of LEDs active area, which resulted in a PDMS/SiN composite coating with thickness of about

$500\ \mu\text{m}$ (Fig. 2(a), step 8). PDMS curing of the as-modified LEDs is then carried out at 60°C for 4 h.

An optical spectrophotometer is used for measurement of LED's spectral radiance in the visible region ($380\text{ nm} - 780\text{ nm}$), both before and after modification with red-emitting SiNs. For all the tested LEDs, spectral radiance data are collected for different values of the bias current (40, 60, 80, 100, and 120 mA) and for two different solid angles (0.1° and 1°). By changing the measurement angles, it is possible to change the size of the measurement area, which corresponds to a circular area with diameter of 0.1 mm and 1.0 mm for angles of 0.1° and 1° , respectively, at working distance of 7 cm. Spectral radiance allows to infer on photoluminescence properties of SiNs upon stimulation with the excitation light of blue-LEDs (centered at $\lambda = 450\text{ nm}$), as well as to compute x and y color coordinates and, in turn, to infer on color of SiN-modified LEDs.

Figure 4 shows typical normalized radiance spectra of commercial blue LEDs before (Fig. 4(a)) and after (Figs. 4(b)–4(d)) modification with $5\ \mu\text{l}$ of PDMS encapsulating different SiN concentrations, as a function of the LED's bias current. The spectra in Fig. 4 refer to measurements taken within a solid angle of 0.1° and averaged over several measurements carried out both on same and different LEDs. Measurements taken using a solid angle of 1° yield similar

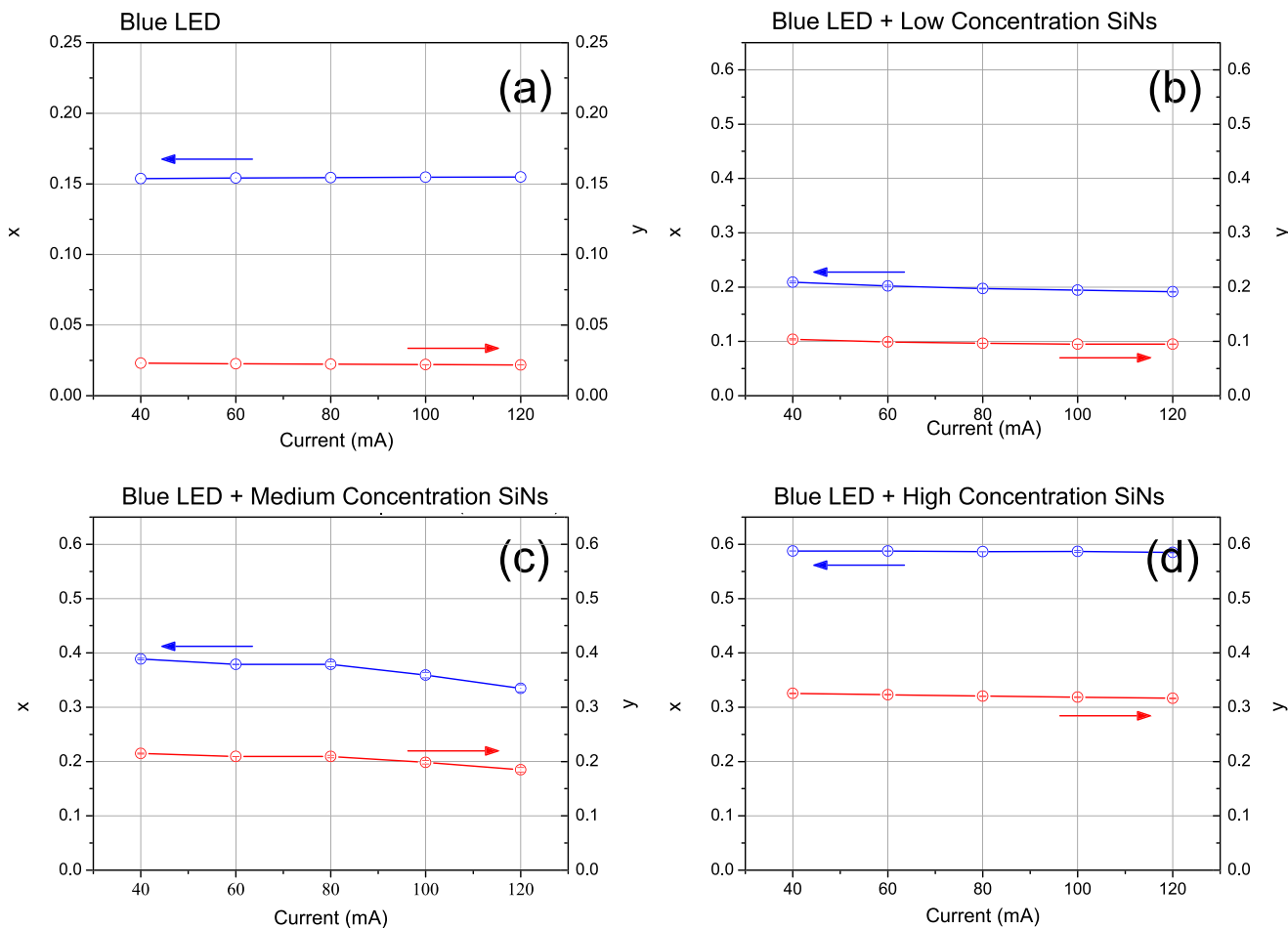


FIG. 5. Color coordinates x and y (average value and standard deviation, this latter non-visible being smaller than the dots representing the average value) of unmodified (a) and SiN-modified ((b)–(d)) LEDs for different SiN concentrations, as a function of the LEDs bias current.

results. Possible contribution of PDMS to modification of the emission spectrum is ruled out by comparison of the spectral radiance of unmodified blue-LEDs and blue-LEDs coated with 5 μl of bare PDMS without SiNs (see supplementary material²⁵). The commercial blue-LEDs features a radiance spectrum with a single emission band centered at 450 nm with full-width at half maximum (FWHM) of 17 nm (Fig. 4(a)). The radiance spectra of LEDs modified with SiNs exhibit two emission bands, one in the blue part of the visible range mainly due to the blue-LED emission and one in the red part of the visible range due to SiN emission upon excitation with the blue-LED light. The red emission band is centered around 670 nm with FWHM of about 120 nm (Figs. 4(c) and 4(d)), which corresponds to photoluminescence of SiNs with average size of 2.9 nm, based on the assumption that quantum confinement effects dominate the observed photoluminescence.^{12,26,27} Although most of the SiNs of the network show orange-red luminescence, a number of nanocrystals in the silicon network seems to feature blue luminescence, and thus smaller size, which explains changes on the line-shape of the blue-band in radiance spectra of LEDs modified with SiNs, with respect to that of the non-modified blue-LED. Best-fitting of radiance spectra of LEDs modified with different concentrations of SiNs using a three-Gaussian-curves deconvolution approach allows to clearly identify the blue luminescence contribution, centered around 470 nm with FWHM of 35 nm, that originates from SiNs with size around 1.8 nm, upon blue-LED excitation (see supplementary material²⁵). Nonetheless, blue luminescence contribution originating either from localized states in the silicon oxide shell or at the oxide/silicon interface of partially oxidized SiNs cannot be ruled out.²⁸

Figures 4(a)–4(d) clearly highlight that the more the SiN concentration the more the portion of the blue emission that is down-converted into red-light, thus changing the color appearance of the LED from blue to violet, magenta, and red as the SiN concentration increases. In particular, blue-LEDs modified with low-concentration of SiNs show an emission spectrum (Fig. 4(b)) with a still dominant blue band; blue-LEDs modified with medium-concentration of SiNs show comparable relative radiance values of blue and red emission bands (Fig. 4(c)); blue-LEDs modified with high-concentration of SiNs show a dominant red band (Fig. 4(d)). The LED bias current only affects the intensity of blue and red emission-bands, which linearly increases with the bias current for all the SiN concentrations (see supplementary material²⁵) while preserving the radiance spectrum line-shape. Noteworthy, an excellent stability of the color of SiN-modified LEDs with the LED bias current is achieved for all the SiN concentrations, as shown in Figure 5 in which no significant variations of x and y color coordinates and, in turn, of LED color of SiN-modified LEDs is observed as the bias current is increased from 40 to 120 mA.

Concluding, in this work, we demonstrate that nanostructured forms of silicon, specifically red-emitting SiNs embedded into a silicon network obtained by partial electrochemical erosion of silicon in acidic electrolyte, can be effectively used as non-toxic phosphor for tuning the color

of commercial LEDs by changing the SiN concentration. Good reliability of the tuning process, with respect to SiN synthesis, and excellent stability of the tuning color, with respect to LEDs bias current, are demonstrated, thus envisaging stimulating perspectives in the field of light-emitting applications of SiNs.

Authors would like to thank staff at ST Microelectronics, Milan (Italy), for SEM images of samples with SiN networks as well as R.I.CO. s.r.l. for partially funding this work.

- ¹L. Mangolini, *J. Vac. Sci. Technol. B* **31**, 020801 (2013).
- ²L. T. Canham, *Appl. Phys. Lett.* **57**, 1046 (1990).
- ³S.-M. Liu, Y. Yang, S. Sato, and K. Kimura, *Chem. Mater.* **18**, 637 (2006).
- ⁴X. D. Pi, R. W. Liptak, J. Deneen Nowak, N. P. Wells, C. B. Carter, S. A. Campbell, and U. Kortshagen, *Nanotechnology* **19**, 245603 (2008).
- ⁵J. Zou, P. Sanelle, K. A. Pettigrew, and S. M. Kauzlarich, *J. Cluster Sci.* **17**, 565 (2006).
- ⁶S. S. Walavalkar, C. E. Hofmann, A. P. Homyk, M. D. Henry, H. A. Atwate, and A. Scherer, *Nano Lett.* **10**, 4423 (2010).
- ⁷K.-Y. Cheng, R. Anthony, U. R. Kortshagen, and R. J. Holmes, *Nano Lett.* **11**, 1952 (2011).
- ⁸R. J. Anthony, K.-Y. Cheng, Z. C. Holman, R. J. Holmes, and U. R. Kortshagen, *Nano Lett.* **12**, 2822 (2012).
- ⁹F. Maier-Flaig, J. Rinck, M. Stephan, T. Bocksrocker, M. Bruns, C. Kübel, A. K. Powell, G. A. Ozin, and U. Lemmer, *Nano Lett.* **13**, 475 (2013).
- ¹⁰K.-Y. Cheng, R. Anthony, U. R. Kortshagen, and R. J. Holmes, *Nano Lett.* **10**, 1154 (2010).
- ¹¹D. P. Puzzo, E. J. Henderson, M. G. Helander, Z. Wang, G. A. Ozin, and Z. Lu, *Nano Lett.* **11**, 1585 (2011).
- ¹²M. L. Mastronardi, F. Maier-Flaig, D. Faulkner, E. J. Henderson, C. Kübel, U. Lemmer, and G. A. Ozin, *Nano Lett.* **12**, 337 (2012).
- ¹³B. Gelloz, A. Kojima, and N. Koshida, *Appl. Phys. Lett.* **87**, 031107 (2005).
- ¹⁴C.-C. Tu, Q. Zhang, L. Y. Lin, and G. Cao, *Opt. Express* **20**, A69 (2011).
- ¹⁵C.-C. Tu, J. H. Hoo, K. F. Bohringer, L. Y. Lin, and G. Cao, *Opt. Lett.* **37**, 4771 (2012).
- ¹⁶S. Nakamura, M. Senoh, and T. Mukai, *Appl. Phys. Lett.* **62**, 2390 (1993).
- ¹⁷J. S. Kim, P. E. Jeonny, J. C. Choi, H. L. Park, S. I. Mho, and G. C. Kim, *Appl. Phys. Lett.* **84**, 2931 (2004).
- ¹⁸S. Neeraj, N. Kijima, and A. K. Cheetham, *Chem. Phys. Lett.* **387**, 2 (2004).
- ¹⁹T. Nakajima, M. Isobe, T. Tsuchiya, Y. Ueda, and T. Kumagai, *Nat. Mater.* **7**, 735 (2008).
- ²⁰V. L. Colvin, M. C. Schlamp, and A. P. Alvisatos, *Nature* **370**, 354 (1994).
- ²¹J. Lee, V. C. Sundar, J. R. Heine, M. G. Bawendi, and K. F. Jensen, *Adv. Mater.* **12**, 1102 (2000).
- ²²V. Wood, M. J. Panzer, J. Chen, M. S. Bradley, J. E. Halpert, M. G. Bawendi, and V. Bulovic, *Adv. Mater.* **21**, 2151 (2009).
- ²³Y. Shirasaki, G. J. Supran, M. G. Bawendi, and V. Bulović, *Nat. Photon.* **7**, 13 (2013).
- ²⁴V. Lehmann, *Electrochemistry of Silicon—Instrumentation, Science, Materials and Applications* (Wiley-VCH, 2002).
- ²⁵See supplementary material at <http://dx.doi.org/10.1063/1.4867201> for Figure S1, experimental data on preparation of silicon nanocrystal layers; Figure S2, spectral radiance of LEDs uncoated and coated with 5 μl of bare PDMS (without SiNs), and best-fitting of radiance spectra of LEDs modified with low-concentration SiNs using three Gaussian curves; Figure S3, intensity of the wavelength peak of both blue and red emission bands versus bias current for both unmodified LEDs and LEDs modified with different concentrations of SiNs.
- ²⁶J. R. Rodríguez Nuñez, J. A. Kelly, E. J. Henderson, and J. G. C. Veinot, *Chem. Mater.* **24**, 346 (2012).
- ²⁷D. C. Hannah, J. Yang, P. Podsiadlo, M. K. Y. Chan, A. Demortière, D. J. Gosztola, V. B. Prakapenka, G. C. Schatz, U. Kortshagen, and R. D. Schaller, *Nano Lett.* **12**, 4200 (2012).
- ²⁸B. Gelloz, R. Mentek, and N. Koshida, *Jpn. J. Appl. Phys.* **48**, 04C119 (2009).